Flow Property Measurement Using Laser-induced Fluorescence in the NASA Ames Interaction Heating Facility

Jay H. Grinstead*
NASA Ames Research Center, Moffett Field, CA 94035

Barry J. Porter†
AerospaceComputing, Inc., Moffett Field, CA 94035

J. Enrique Carballo‡
NASA Ames Research Center, Moffett Field, CA 94035

The spectroscopic diagnostic technique of two photon absorption laser-induced fluorescence (TALIF) of atomic species has been applied to single-point measurements of velocity and static temperature in the NASA Ames Interaction Heating Facility (IHF) arc jet. Excitation spectra of atomic oxygen and nitrogen were recorded while scanning a tunable dye laser over the absorption feature. Thirty excitation spectra were acquired during 8 arc jet runs at two facility operating conditions; the number of scans per run varied between 2 and 6. Curve fits to the spectra were analyzed to recover their Doppler shifts and widths, from which the flow velocities and static temperatures, respectively, were determined. An increase in the number of independent flow property pairs from each as-measured scan was obtained by extracting multiple lower-resolution scans. The larger population sample size enabled the mean property values and their uncertainties for each run to be characterized with greater confidence. The average $\pm 2\sigma$ uncertainties in the mean velocities and temperatures for all 8 runs were ±1.4% and ±11 %, respectively.

I. Introduction

High enthalpy arc-heated and plasma facilities simulate the aerothermal heating environment encountered by hypervelocity and atmospheric entry vehicles. These facilities are used for screening, evaluation, and acceptance testing of thermal protection materials. Accurate knowledge of facility performance is critical for understanding the differences between the ground test and flight environments, validating high-fidelity computational simulations of the test environment, and designing experiment protocols to meet program requirements[1]. Development of optical techniques for characterizing these facilities of has been an active area of research for many years.[2,3] Emission, laser absorption, and laser-induced fluorescence spectroscopy techniques have been applied for measurements of atomic and molecular species.[4-18] The quantities measured can be related to gas dynamic and thermochemical properties of the free stream, such as temperature, velocity, species concentrations, enthalpy, as well as revealing the degree thermochemical nonequilibrium.[5-7]

Laser-induced fluorescence (LIF) of atomic oxygen and nitrogen has proven to be a powerful technique for flow property measurements in the NASA Ames Aerodynamic Heating Facility,[4-8] a 20 MW large-scale arc jet. The number of LIF systems devoted to arc-heated and plasma facilities has expanded in the last several years in the United States,[9] Europe,[10-13] and Japan.[14-16] A new, state-of-the-art LIF system was developed for the 60 MW Interaction Heating Facility (IHF) arc jet[19] at Ames. After a series of integrated systems tests, the IHF LIF system was used in a dedicated facility characterization test series.

Unlike laboratory or small-scale test facilities, the Ames arc jets require significant commitment of resources for their operation. Test runs are scheduled and highly scripted to minimize the amount of arc-on time necessary to meet test objectives. Improvised evaluation and optimization of LIF system performance, while often appropriate in laboratory or small-scale facilities, is not a prudent use of an expensive facility. The design of the IHF LIF system was

* Senior Research Scientist, Aerothermodynamics Branch, MS 230-2, Associate Fellow AIAA
† Research Engineer, Experimental Aero-Physics Branch, MS 260-1, Member AIAA
‡ Mechanical Engineer, Thermophysics Facilities Branch, MS 229-4

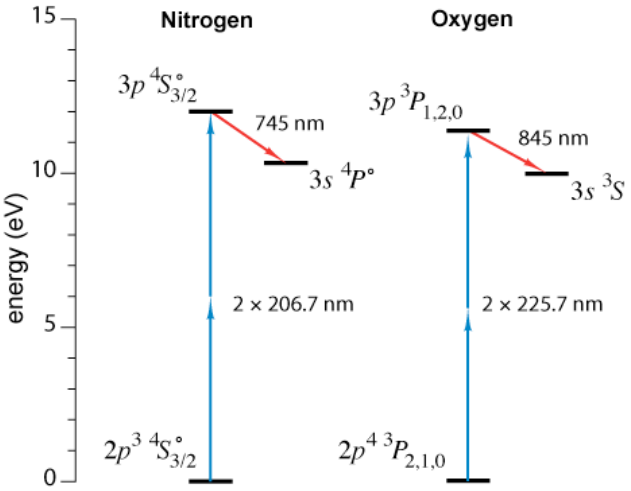

Figure 1. Excitation and emission paths and participating electronic states for two photon laser-induced fluorescence of atomic nitrogen and oxygen.

motivated by the need to maximize utility of and minimize effort devoted to instrument operation. The data obtained from this test series was used to evaluate data acquisition and analysis methods. In this paper, we report the first free stream temperature and velocity measurements obtained with LIF of atomic oxygen and nitrogen in the IHF arc jet. Uncertainties in the flow properties were also characterized using two different data reduction approaches. The results will aid in optimizing instrument performance and establishing best practices for future LIF measurements.

II. Arc jet flow property measurement using laser-induced fluorescence

Two photon absorption LIF (TALIF) spectroscopy and its application to nonintrusive gas-phase diagnostics for arc jet flows have been described previously.[4-8,20] Light from a tunable ultraviolet laser source excites the targeted atomic species through the simultaneous absorption of two photons. The excited state emits, or fluoresces, a near-infrared photon as it decays to an intermediate state. The emitted fluorescence is imaged onto a photodetector, and the fluorescence signal is recorded as the tunable laser is scanned over the absorption feature. The magnitude of the fluorescence signal, integrated in wavelength across the scanned absorption feature, is proportional to the number density of the absorbing state and the square of the incident laser pulse energy. The proportionality constant is a product of several spectroscopic, geometric, and experimental factors and is determined through calibration.[4-8,13,21,22] The TALIF processes for atomic oxygen and atomic nitrogen are shown in Fig. 1.

A schematic of the TALIF application to an arc jet flow is shown in Fig. 2. The excitation beam crosses the flow axis at a non-normal angle. The fluorescence excited along the beam path is collected from a small volume defined by the intersection of the laser beam and the region subtended by the collection optics. The probe volume is aligned to a point on the flow axis at a prescribed distance from the nozzle exit. The fluorescence collected from this volume is imaged onto a photodetector equipped with spatial, spectral, and neutral density filters. The magnitude of the fluorescence signal and its temporal decay are recorded as the laser is scanned over the absorption feature. The measured excitation lineshape is analyzed to determine the Doppler shift in the absorption waßvelength, Doppler width, and integrated signal intensity, from which the flow velocity, temperature, and absolute species density, respectively, can be recovered.[4-8,20]

Accurate analysis of the TALIF excitation line shape is critical to extracting temperature and velocity from the

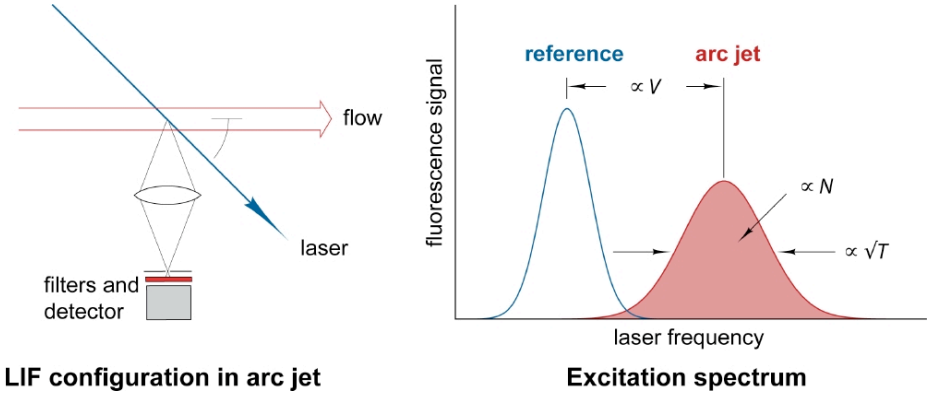

Figure 2. Simultaneous property measurement in the arc jet free stream from the laser-induced fluorescence excitation spectrum. Velocity is obtained from the frequency shift of the absorption feature. Temperature is obtained from the Doppler broadening of the excitation line shape.

laser scans. A stable source of atomic oxygen and nitrogen atoms in the laboratory was created using a microwave discharge flow reactor system. The source enabled TALIF measurements under controlled conditions. Line shape measurements obtained in the flow reactor were used as references to similar measurements in the arc jet facility. The source is described in Section III.

The line shape observed from two photon excitation is a convolution of the absorption line shape and the autocorrelation of the laser spectral profile.[20] The dominant line-broadening mechanism at the thermodynamic conditions encountered in the flow reactor and arc jet is thermal (Doppler); collisional, Stark (electron/ion-induced), and power (laser-induced) broadening were estimated to be negligible. Gaussian line shape functions were therefore used for the absorption features. The laser spectral profile was determined to be Gaussian from analysis of the adjacent TALIF excitation line shapes of krypton and xenon[21,22] at the low pressures of the laboratory source. The relatively large atomic masses of krypton and xenon result in negligible thermal broadening at ambient temperature, and the observed TALIF line shapes were fit well by Gaussian line shape functions.

With both the absorption feature and laser spectral profile approximated by Gaussian line shape functions, the two photon excitation line shape function is also Gaussian. The parameters of interest are the line center wavelength, λ_0, and the total full-width half-maximum (FWHM) line width, $\Delta\lambda_{tot}$,

$$\Delta\lambda_{tot} = \sqrt{\Delta\lambda_D^2 + 2\Delta\lambda_L^2} \tag{1}$$

where $\Delta\lambda_D$ is the Doppler width and $\Delta\lambda_L$ is the laser line width. The factor 2 of arises from the autocorrelation of the laser spectral profile.[20] The Doppler width is a function of the temperature T and atomic mass M,

$$\Delta\lambda_D = \frac{\lambda_0}{c}\sqrt{8\ln 2\frac{kT}{M}} \tag{2}$$

where c is the speed of light and k is Boltzmann's constant.

The laser line width can be extracted from the total width of a Gaussian curve fit to the excitation spectrum measured in the flow reactor. The Doppler width is computed using the measured temperature of the flow reactor T_{fr}. The laser line width is computed from Eq. (1) using the total line width,

$$\Delta\lambda_L = \sqrt{\frac{\Delta\lambda_{tot,fr}^2 - \Delta\lambda_{D,fr}^2}{2}} \tag{3}$$

where the subscript *fr* refers to quantities of the flow reactor excitation spectrum.

The Doppler width from the arc jet excitation spectrum is computed from the measured total line width and the laser line width

$$\Delta\lambda_{D,aj} = \sqrt{\Delta\lambda_{tot,aj}^2 - 2\Delta\lambda_L^2}\,. \tag{4}$$

Here, the subscript *aj* refers to the quantities of the arc jet excitation spectrum. Eqs. (3) and (4) can be combined to yield $\Delta\lambda_{D,aj}$ in terms of the measured total line widths,

$$\Delta\lambda_{D,aj} = \sqrt{\Delta\lambda_{tot,aj}^2 - \Delta\lambda_{tot,fr}^2 + \Delta\lambda_{D,fr}^2}\,. \tag{5}$$

Finally, the temperature of the arc jet free stream T_{aj} was computed from $\Delta\lambda_{D,aj}$ using the inversion of Eq. (2),

$$T_{aj} = \frac{1}{8\ln 2}\frac{Mc^2}{k}\left(\frac{\Delta\lambda_{D,aj}}{\lambda_0}\right)^2. \tag{6}$$

The temperature is proportional to the square of the Doppler width and thus is particularly sensitive to uncertainties in the fitted parameters $\Delta\lambda_{tot,fr}$ and $\Delta\lambda_{tot,aj}$.

The flow velocity vector $\mathbf{V}_{aj}$ induces a Doppler shift $\delta\nu$ of the arc jet transition frequency line center ν_0,

$$\delta\nu = -\frac{\nu_0}{c}\mathbf{V}_{aj}\cdot\mathbf{i}_L \tag{7}$$

where $\mathbf{i}_L$ is the unit vector of the laser beam path.[8] In terms of the arc jet and flow reactor transition center wavelengths, the magnitude of the arc jet velocity vector at the measurement location is

$$V_{aj} = \frac{c}{\cos(\theta)}\frac{\lambda_{0,aj} - \lambda_{0,fr}}{\lambda_{0,fr}} \tag{8}$$

where θ is the angle between the laser beam vector and the arc jet nozzle center line, which is presumed to be parallel to $\mathbf{V}_{aj}$.

In summary, the six quantities needed to determine the arc jet temperature and velocity are $\lambda_{0,fr}$, $\Delta\lambda_{tot,fr}$, $\lambda_{0,aj}$, $\Delta\lambda_{tot,aj}$, T_{fr}, and θ. The uncertainties of each can be characterized; the uncertainties in the flow properties can thus be computed by propagating these uncertainties through the constitutive expressions derived above.

III. Experimental configuration

The IHF arc jet, with a 60 MW arc heater, is the largest and most powerful arc jet facility operating within NASA. The IHF's arc heater operates with air/argon test gas mixtures. The heater produces enthalpies from 7 to 50 MJ/kg, The facility can be configured with conical nozzles with exit diameters from 15 cm to 104 cm for free jet flows, or a semi-elliptic nozzle for wall-bounded shear flows. The IHF LIF system is comprised of several major subsystems, each of which was described in detail previously.[19] For completeness, the relevant subsystems will be described briefly below.

A. Laser system and laboratory optical configuration

The laser system is a pulsed tunable dye laser that is frequency tripled to reach ultraviolet wavelengths between approximately 204 nm and 230 nm. A frequency doubled, injection-seeded Nd:YAG laser, operating at 20 Hz, is used to pump the dye laser. The maximum pulse energy of the frequency-tripled dye laser output is approximately 4 mJ, and the pulse duration and spectral bandwidth are approximately 5 ns and 0.15-0.2 cm^{-1}, respectively. The laser dye used for the N LIF measurements was Rhodamine 640, while LDS 698 was used for the O LIF measurements. A high-energy variable attenuator permits continuous control over the pulse energy. Approximately 20% of the UV laser beam pulse energy is reserved for frequency and LIF calibration measurements in the laboratory. The remaining 80% is directed out of the laboratory to the arc jet test cabin. Losses along the transmission path to the measurement location, primarily due to the multiple turning elements, reduce the maximum pulse energy to approximately 750 μJ.

B. Laboratory flow reactor calibration source

The laboratory source of atomic species was required as an absorption frequency reference for the Doppler shift and width measurements extracted from excitation profiles measured in the arc jet. The flow apparatus was constructed from quartz tubing and fittings, and mass flow controllers regulated prescribed flow rates of gases admitted to the flow reactor. A pressure controller and downstream throttle valve maintained a prescribed pressure in the flow reactor. A 2.45 GHz microwave generator drives a cylindrical resonator surrounding the quartz tube inlet arm of the flow reactor. The generator drives the resonator at 60 W and dissociates a small fraction (approximately 0.2-1.0%) of a metered N_2 or O_2 flow buffered with helium. The apparatus has optical access windows for the probe beam and fluorescence collection. A thermocouple attached near the observation window monitors the gas temperature. Typical operating pressures were 0.5 to 1.0 torr (6.65 to 13.3 Pa).

Laser wavelength calibration was also accomplished using the flow system. Laser wavelengths of adjacent TALIF transitions of atomic krypton and xenon[21,22] were measured by introducing buffered mixtures of these gases in the flow reactor. Curve fits of the absolute vs. observed transition wavelengths of N and Kr were used to correct the laser wavelength scale for subsequent Doppler width and shift analyses of N LIF scans obtained in the arc jet. The same approach was used with O and Xe transitions for width and shift analyses O LIF scans.

C. Integrated optical receiver

The flow reactor and arc jet LIF signals were collected with integrated receiver systems. Each receiver includes secondary imaging optics; spatial, spectral, and neutral density filters; a photodetector; and signal amplification. An

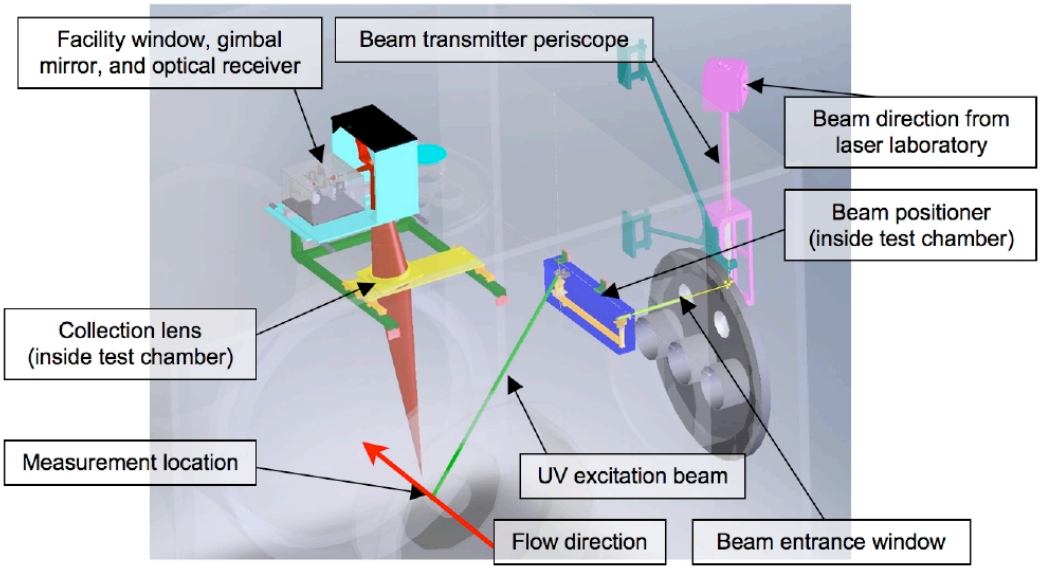

Figure 3. Rendering of LIF system beam transmitter and optical receiver hardware for the IHF arc jet test cabin.

aperture at the focus of the primary collection optics restricts the extent of the imaged region of the excitation laser beam to 3 mm and 6 mm for the laboratory and arc jet configurations, respectively. Secondary optics within the receiver collimate the fluorescence to pass through a filter assembly and focus on the photodetector. The filter assembly consists of two motorized filter wheels with neutral density and narrowband (~40 nm) spectral filters, respectively. The center wavelengths of the pass bands of the spectral filters were chosen to coincide with the fluorescence wavelengths of the targeted LIF species (N, O, Kr, Xe), which are in the near infrared.[21,22]

D. Arc jet optical configuration

The optical configuration for the IHF test cabin was configured for single-point TALIF measurements on the flow centerline. A perspective rendering of the IHF arc jet test cabin and the LIF beam transmitter and optical receiver components is shown in Fig. 3. The beam from the laboratory is directed downward through a two-lens telescope, turned horizontally, and enters the test cabin through a dedicated window. Mounted on the inside wall of the test cabin is an enclosed beam positioner that catches the beam after it passes through the window. The positioner directs the beam upstream to intersect the nozzle axis 10" (25.4 cm) downstream of the exit. The beam diameter at the probe volume is approximately 1 mm. The standoff distance from the final turning mirror on the positioner to the probe volume was 1.74 m.

The probe volume was defined by the intersection of the beam and collection cone of the imaging optical path. The primary objective of the collection optics was attached to a truss mounted to the ceiling inside the test cabin. The lens focused the fluorescence from the probe volume through a window on the ceiling of the test cabin. The standoff distance from the objective lens to the probe volume was 0.85 m. A mirror located above the window directs the imaged fluorescence horizontally to an integrated optical receiver.

E. Experiment control and data acquisition

An integrated LabVIEW and MATLAB software solution was developed to remotely operate all subsystems of the experiment and record data. The primary quantities of interest for the arc jet temperature and velocity measurements reported here are the LIF signals from the laboratory flow reactor and arc jet. A 5 Gs/s digital oscilloscope was used to acquire the time-resolved LIF signals as the laser was stepped in wavelength over the absorption transitions. The recorded data products are two-dimensional matrices of LIF signal magnitude vs. laser wavelength and vs. time, i.e. $S_{LIF}(\lambda_L, t)$. The flow reactor and arc jet LIF signal channels were recorded simultaneously. For N LIF measurements, the flow reactor was operated with a mixture of He and N_2 partially dissociated by the microwave discharge; similarly for O LIF, the microwave discharge partially dissociated an O_2/He mixture. Pulse averaging was employed to improve the signal-to-noise ratio at each laser wavelength step. For the data recorded for this test series, the wavelength step size was 0.0004 nm, and 10 pulses were averaged at each wavelength step.

Table 1. IHF operating parameters

Test condition	C1 (low)	C2 (high)
Current (A)	1980	5980
Voltage (V)	3840	7010
Pressure (kPa)	240	890
Air flow rate (g/s)	200	740
Ar flow rate (g/s)	21	54
Add-air flow rate (g/s)	55	55
Bulk enthalpy (MJ/kg)	14.9	26.6

Table 2. TALIF measurement test matrix

Run number	Test condition	LIF species	Number of scans
1	C2	N	2
5	C1	N	3
6	C1	N	4
7	C1	N	6
8	C2	N	3
10	C2	N	4
11	C2	O	3
12	C2	O	5

IV. Results

The TALIF measurements of flow properties were conducted during a test series devoted to facility characterization. The IHF was configured with a 13" (33 cm) nozzle exit diameter. Two test conditions were chosen for this test series. Test condition 1 (C1) generated a moderate (14.9 MJ/kg) average enthalpy. The enthalpy for condition 2 (C2) was towards the higher end of the facility range (26.6 MJ/kg). The nominal arc jet heater operating parameters and enthalpies are listed in Table 1.

TALIF data were obtained during eight runs of the test series. Since the laser dyes used for TALIF of N and O were different, the laser system needed to be reconfigured when changing target species. Therefore, TALIF measurements for each run were for either atomic N or O. The first six runs were dedicated for N LIF. The laser configuration was then changed, and the last two runs were dedicated for O LIF. The number of laser scans per run varied between two and six and depended on available time during the run. The total number of scans obtained over the test series was 30. Table 2 shows the matrix of run conditions, target species, and number of measurements for the eight runs in which LIF was employed.

The LIF signal data matrices for the flow reactor and arc jet channels were integrated in time over the duration of the fluorescence pulses to yield excitation spectra vectors as functions of laser wavelength. Curve fits to the excitation spectra yielded their respective transition line centers and line widths. As described in Section II, these values were then used to compute the temperature and velocity of the arc jet free stream at the measurement location.

A. Line shape analysis

The ground and excited electronic states of the two photon absorption transition for nitrogen, $3p^3\,{}^4S_{3/2} \leftarrow 2p^3\,{}^4S_{3/2}$ have no fine structure. The observed line shape is represented by a single Gaussian line shape function. Unlike the nitrogen atom, however, the oxygen atom ground and excited electronic states coupled by two photon absorption do have fine structure. The ground state, $2p^4\,{}^3P_J$, is split into three levels, each of which is coupled to the three levels of the $3p\,{}^3P_J$ upper state. The absorption cross section for transitions from the $J''(2)$ (lowest energy) ground state fine structure level to the $3p\,{}^3P_J$ upper state were the largest of the three.[23] The splitting of the upper state J' fine structure levels relative to their Doppler widths was sufficiently large that the three transitions from $J''(2)$ were partially resolved. The relative absorption cross sections and frequency differences of the three transitions were obtained from the theoretical analysis of Saxon et. al.[24] Figure 4 shows an excitation spectrum of the $J'(1,2,3) \leftarrow J''(2)$ triplet obtained in the flow reactor at a total mixture pressure of 1.0 torr (13.3 Pa) and temperature of 323 ± 5 K. The curve fit to the spectrum is a superposition of the fine structure components, with the relative magnitudes of each Gaussian line shape component weighted by their relative cross sections. The Doppler broadening of each component was computed according to Eq. (2). Also shown is a bar representing the laser line width determined from the curve fit.

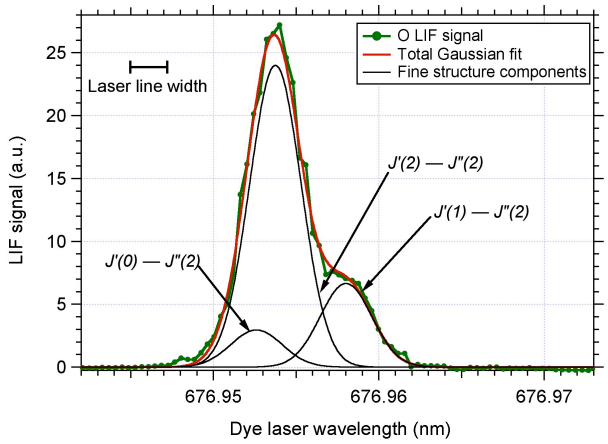

Figure 4. Excitation spectrum of atomic oxygen and its curve fit obtained in the laboratory flow reactor at a temperature of 323 ± 5 K. The laser line width, determined from the curve fit, is also shown.

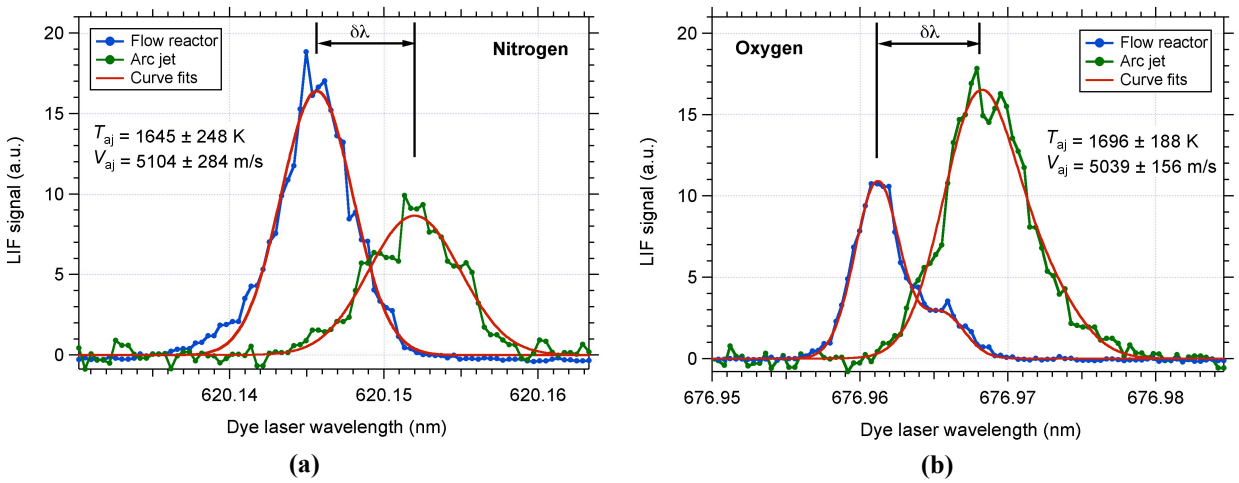

Figure 5. Excitation spectra and their curve fits obtained in the laboratory flow reactor and arc jet at test condition C2. The Doppler shift δλ and Doppler width were used to determine the velocity and temperature, respectively, of the arc jet free stream. The flow property uncertainties are ± 2σ values propagated from 95% confidence limits of the fitted shifts and widths. (a) Nitrogen. (b) Oxygen.

B. Statistical determination of flow properties

The 30 excitation spectra pairs obtained during the arc jet runs were analyzed to recover the relevant curve fit parameters: $\lambda_{0,fr}$, $\Delta\lambda_{tot,fr}$, $\lambda_{0,aj}$, and $\Delta\lambda_{tot,aj}$. Examples of spectra and curve fits for N and O at test condition C2 are shown in Figs. 5a and 5b, respectively. The temperatures and velocities computed from the fitted parameters are also noted in each figure. The 95% confidence limits of the fitted parameters were estimated from the goodness-of-fit statistics of the nonlinear regression analysis. These limits, along with estimated uncertainties of T_{fr}, and θ, were used to compute the $\pm 2\sigma$ uncertainties of the temperature and velocity for each measured spectrum. The uncertainties propagated in this manner apply only to individual measurements and not the mean of multiple, independent measurements.

Since the number of scans per run was small (between two and six), however, statistical estimation methods do not provide meaningful insight into probability distributions of the flow properties determined from those scans. An increase in sample size is necessary to compute statistically significant moments (mean, standard deviation of the mean) of the measured flow property population for each run. This may be accomplished by extracting multiple sparse spectra by sampling equally-spaced points from one scan without resampling. In effect, a high resolution excitation spectrum is considered to consist of several interleaved but independent lower resolution excitation spectra, each of which can be analyzed. The number of points across the feature must be sufficient to obtain a viable curve fit, however. This data reduction and analysis approach was explored with the 30 scans of the test series.

The sparse spectra extracted from the original spectra have effectively larger wavelength step sizes. The consequences of increasing the wavelength step size on the curve fit parameters (and the flow properties computed from them) were examined with one of the excitation spectra pairs. The effective step sizes were increased by integer factors of 2 through 10 (0.0008 nm to 0.004 nm), with the same factor decrease in the number of points in the spectra. The modified spectra were then analyzed following the same curve fitting procedure described above. The O LIF spectra of Fig. 5b were used to demonstrate the results of increasing step size. Figure 6 shows one example, where the spectra were sampled to a step size of 0.002 nm (5x increase). The curve fits and the flow properties computed from the fit parameters are also shown. Even with only 20% of the points, the property values are within 6% of those from the original spectra, indicating that a small number of points is sufficient to characterize the line shape. The results of sampling the original spectra are summarized in Fig. 7, where flow properties and their derived $\pm 2\sigma$ uncertainties are plotted vs. effective step size. The ranges of fitted laser line width and $\Delta\lambda_{tot,fr}$ are indicated for comparison with the wavelength step size. The arc jet feature width, $\Delta\lambda_{tot,aj}$, at ~0.0057 nm is beyond the scale of the plots. The viability of the curve fit breaks down as the step size reaches the total flow reactor line width: the number of points in the spectrum that defines that line shape is too few, and the fitted curve no longer approximates

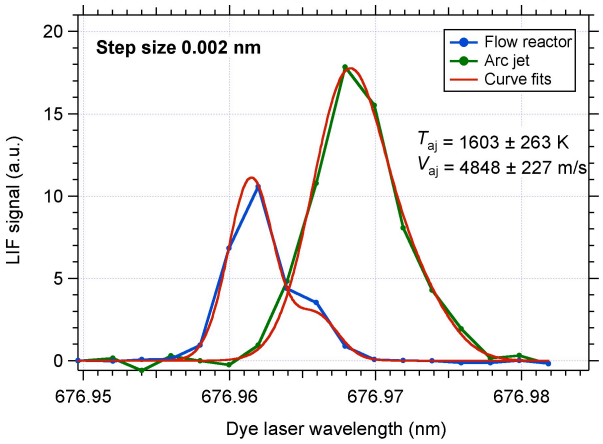

Figure 6. Excitation spectra of Fig. 5b after sampling with an effective laser wavelength step size 0.002 nm. Curve fits, and the arc jet flow properties determined from them, are also shown.

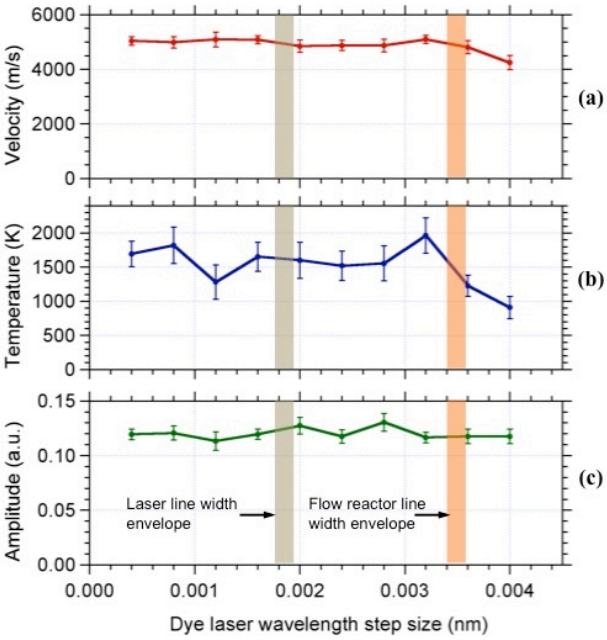

Figure 7. Variation of flow properties with effective dye laser wavelength step size computed from curve fits to increasingly sparse spectra extracted from the as-measured spectra (Fig. 5b). The envelopes of fitted laser and total flow reactor line widths are indicated.

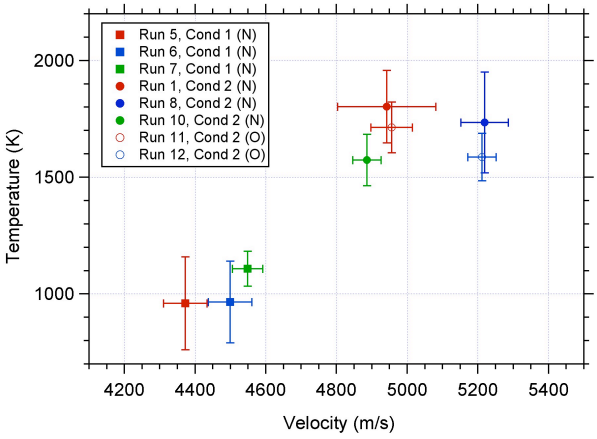

Figure 8. Average temperatures and velocities for the eight arc jet runs using the second data reduction method (see text). The error bars denote the $\pm 2\sigma_m$ uncertainties in the sample mean values.

the original spectrum. The temperature and velocity, which depend on $\Delta\lambda_{tot,fr}$, deviate from their values at larger wavelength step sizes. Also plotted in Fig 7c is the leading amplitude parameter of the fitted arc jet line shape function; this factor is proportional to the integral of the excitation line shape and would be used for measurements of absolute species density.[8] Because the arc jet feature is appreciably wider than the flow reactor feature, it can be fitted successfully at larger effective wavelength step sizes. It is apparent that significant wavelength step size increases are possible without compromising the integrity of the curve fits.

With a recorded spectrum of fixed length, the number of sparse spectra that can be extracted increases in proportion to the chosen wavelength step size. For example, five unique sparse spectra can be extracted when every fifth point in the original spectra are sampled, thus yielding a five-fold increase in the number of flow property measurements. All data points in the recorded spectrum are used, but only once. The 30 scan pairs of the test series were processed using this approach. Rather than only 2 to 6 independent property measurements per arc jet run, the number of measurements increased to 10 to 30. While not large, these sample sizes are sufficient to apply an estimation method to determine the mean and the standard deviation of the mean (or standard error, σ_m). Figure 8 shows the mean values of flow properties for each run. The error bars denote the $\pm 2\sigma_m$ uncertainties in the mean values computed from the sample populations. The average uncertainties for all 8 runs were ±1.4% and ±11%, respectively.

Even larger sample sizes can be realized by increasing the total number of laser scans as well as increasing the spectral resolution (smaller wavelength step size) of a single laser scan. Efficient use of arc-on time dominates trade decisions in optimizing the data acquisition protocol. The control parameters are the wavelength step size and the number of pulses to average. Acquisition overhead (experiment control, data manipulation and transfer) adds to the time required to complete one scan. The data acquisition protocol can be optimized to balance the advantages, disadvantages, and risks of few high resolution scan versus many lower resolution scans.

V. Conclusion

Two photon absorption laser-induced fluorescence (TALIF) of atomic oxygen and nitrogen was used for single-point measurements of free stream temperature and velocity in the NASA Ames IHF arc jet. The measurements were obtained in a test series devoted to arc jet characterization. The measurements were acquired during 8 test runs at two facility operating conditions. A total of 30 TALIF excitation spectra pairs (arc jet and laboratory reference) were acquired during the test series. Curve fits to the spectra were performed to determine the Doppler widths and center transition wavelengths of a theoretical line shape function. The Doppler width and shift were used to compute the static temperature and velocity, respectively. Confidence limits of the fitted parameters were also propagated to estimate uncertainties of the flow properties. However, uncertainties from individual measurements do not relate to uncertainties in the average, or mean, of multiple measurements at the same nominal condition. Furthermore, the number of excitation scans per run was small (between 2 and 6), so the number of flow property pairs obtained from fitting each as-measured excitation scan was inadequate to establish meaningful statistics of the mean flow properties for each run. To increase the number of independent flow property pairs obtained from each as-measured scan, multiple lower resolution spectra were extracted from one scan by sampling points from the scan at a fixed interval without reuse. An analysis of curve fits to extracted spectra of decreasing resolution was performed. The analysis indicated that a spectral resolution (sampled wavelength step size) less than the line width of the laboratory reference was sufficient to obtain a viable curve fit. The 30 as-measured excitation spectra of the 8-run data set were analyzed at a factor of 5 decrease in resolution, thus increasing the number of independent flow property pairs obtained per run by a factor of 5. The larger population sample size enabled the mean property values and their uncertainties to be computed with greater confidence. The average $\pm 2\sigma$ uncertainties in the mean velocities and temperatures for all 8 runs were ±1.4% and ±11%, respectively. The advantages of extracting multiple lower resolution spectra for increasing measurement sample size will motivate improvements to experimental procedures.

Acknowledgments

This work was funded in part by the NASA Crew Exploration Vehicle Thermal Protection Systems Advanced Development Project (TPS ADP). Support for the arc jet test series was provided by the Thermophysics Facilities Branch (Dr. George A. Raiche, Chief). The NASA Strategic Capabilities Assets Program (SCAP) provides critical financial support Ames arc jet complex. B. Porter was supported by NASA Contract NAS2-03144 to AerospaceComputing Inc. The authors also thank M. Winter and D. Prabhu for helpful discussions, and the IHF arc jet facility staff for their support during the test series.

References

[1]Grinstead, J.H., Stewart, D.A, and Smith, C.A, "High enthalpy test methodologies for thermal protection systems development at NASA Ames Research Center", AIAA Paper No. 2005-3326, May 2005.

[2]Scott. C.D., "Survey of measurements of flow properties in arcjets", *Journal of Thermophysics and Heat Transfer*, Vol. 7, pp. 9-24, 1993.

[3]Sharma, S.P, Park, C.C., Scott, C.D., Arepalli, S., and Taunk, J., "Arc jet characterization", AIAA Paper No. 1996-0612, Jan. 1996.

[4]Bamford, D.J., O'Keefe, A., Babikian, D.S., Stewart, D.A., and Strawa, A.W., "Characterization of arc-jet flows using laser-induced fluorescence *Journal of Thermophysics and Heat Transfer*, Vol. 9, pp. 26-33, 1995.

[5]Fletcher, D.G, "Arcjet flow properties determined from laser-induced fluorescence of atomic nitrogen", *Applied Optics*. Vol. 38, pp. 1850-1858, 1999.

[7]Fletcher, D.G., "Nonintrusive diagnostic strategies for arcjet stream characterization", *Measurement techniques for high enthalpy and plasma flows*, NATO Research and Technology Organization proceedings RTO-EN-8, 3B-1–3B-37, Neuilly-Sur-Seine Cedex, France, 2000.

[6]Fletcher, D.G., Bamford, D.J., "Arcjet flow characterization using laser-induced fluorescence of atomic species", AIAA Paper No. 98-2458, Jun. 1998.

[8]Grinstead, J.H., Driver, D.M., and Raiche, G.A., "Radial profiles of arcjet flow properties measured with laser-induced fluorescence of atomic nitrogen", AIAA Paper No. 2003-400, Jan. 2003.

[9]Meyers, J.M., Owens, W.P., Dougherty, M., Lutz, A., Uhl, J., and Fletcher, D.G., "Laser spectroscopic investigation of surface-catalyzed reactions for Mars exploration vehicles", AIAA Paper No. 2010-4915, June 2010.

[10]Playez, M., and Fletcher, D.G., "Free stream test conditions determination in ICP wind tunnels using the TALIF measurement technique", AIAA Paper No. 2008-4254, June 2008.

[11]Löhle, S., and Auweter-Kurtz, M., "Inductively heated air plasma flow characterization with laser-induced fluorescence measurements", *Journal of Thermophysics and Heat Transfer*, Vol. 23, No. 1, pp. 208-210, 2009.

[12]Löhle, S., Eichhorn, C., Herdrich, G., and Auweter-Kurtz, M., "Flow characterization using laser-induced fluorescence measurements of atomic nitrogen in inductively heated nitrogen plasma", AIAA Paper No. 2009-4242, June 2009.

[13]Löhle, S., and Auweter-Kurtz, M., "Laser-induced fluorescence measurements of atomic oxygen using two calibration methods", *Journal of Thermophysics and Heat Transfer*, Vol. 21, No. 3, 623-629, 2007.

[14]Mizuno, M., Ito, T., Ishida, K., "Laser induced fluorescence of nitric oxide and atomic oxygen in an arc heated wind tunnel", AIAA Paper No. 2007-4405, June 2009.

[15]Takayanagi, H., Mizuno, M., Fujii, K., Suzuki, T., and Fujita, K., "Arc heated wind tunnel flow diagnostics using laser-induced fluorescence of atomic species", AIAA 2009-1449, Jan. 2009.

[16]Takayanagi, H., Mizuno, M., Fujii, K., Suzuki, T., and Fujita, K., "Arc wind tunnel flow characterization measured by laser-induced fluorescence of atomic species", AIAA 2009-4241, June 2009.

[17]S. Kim, J.B. Jeffries, R.K. Hanson, and G.A. Raiche, "Measurements of Gas Temperature in the Arc-heater of a Large Scale Arcjet Facility using Tunable Diode Laser Absorption, " AIAA Paper No. 2005-900, Jan. 2005.

[18]D.G. Fletcher, G.A. Raiche, and D.K. Prabhu, "A method for determining species mass fractions from spectrally resolved emission measurements", AIAA-2000-2699, 31st AIAA Plasmadynamics and Lasers Conference, Denver, CO (2000).

[19]Grinstead, J.H., Harris, C.L., Yeung, D., Scott, G.P., Porter, B.J., Graube, P., and Greenberg, R.B., "Next-generation laser-induced fluorescence diagnostic systems for NASA arc jet facilities", AIAA Paper No. 2009-1521, Jan. 2009.

[20]Grinstead, J.H., Driver, D.M., and Raiche, G.A., "Optical diagnostics development for the Ames arc jet facilities", AIAA paper 2002-0398, Jan. 2002.

[21]Neimi, K., Schulz-von der Gathen, V., and Döeble, H.F., "Absolute calibration of atomic density measurements by laser-induced fluorescence spectroscopy with two-photon excitation", *Journal of Physics D*, Vol. 34, pp. 2330-2335, 2001.

[22]Neimi, K., Schulz-von der Gathen, V., and Döeble, H.F., "Absolute atomic oxygen density measurements by two-photon absorption laser-induced fluorescence spectroscopy in an RF-excited atmospheric plasma jet", *Plasma Sources Science and Technology*, Vol. 14, pp. 375-386, 2005.

[23]Bamford, D.J., Jusinski, L.E., and Bischel, W.K., "Absolute two-photon absorption and three-photon ionization cross sections for atomic oxygen", *Physical Review A*, Vol. 34, No. 1, pp. 185-198, 1986.

[24]Saxon, R.P., and Eichler, J., "Theoretical calculations of two-photon absorption cross sections in atomic oxygen", *Physical Review A*, Vol. 34, No. 1, pp. 199-206, 1986.